

Published in final edited form as:

*Adv Mater.* 2011 December 15; 23(47): . doi:10.1002/adma.201103316.

## Nanomechanics of Streptavidin Hubs for Molecular Materials

**Dr. Minkyu Kim,**

Department of Mechanical Engineering and Materials Science, Center for Biologically Inspired Materials and Material Systems, Center for Biomolecular and Tissue Engineering, Duke University, Durham, NC 27708, USA

**Dr. Chien-Chung Wang,**

Graduate Institute of Biotechnology, National Chung-Hsing University, Taichung, Taiwan (R.O.C)

**Fabrizio Benedetti,**

Laboratory of Physics of Living Matter, Ecole Polytechnique Fédérale de Lausanne (EPFL), Lausanne, Switzerland

**Dr. Mahir Rabbi,**

Department of Mechanical Engineering and Materials Science, Center for Biologically Inspired Materials and Material Systems, Center for Biomolecular and Tissue Engineering, Duke University, Durham, NC 27708, USA

**Prof. Vann Bennett,** and

Howard Hughes Medical Institute, Department of Biochemistry and Department of Cell Biology, Duke University Medical Center, Durham, NC 27710, USA

**Prof. Piotr E. Marszalek**

Department of Mechanical Engineering and Materials Science, Center for Biologically Inspired Materials and Material Systems, Center for Biomolecular and Tissue Engineering, Duke University, Durham, NC 27708, USA

Piotr E. Marszalek: pemar@duke.edu

---

Polypeptides are used as versatile building blocks for novel biomaterials with many applications.<sup>[1–11]</sup> Typically, protein-based materials are made by randomly cross-linking their monomeric building blocks into supramolecular structures. However, random cross-linking either limits or destroys the advantageous properties of individual proteins, such as their large stretch ratios and structure recovery ability.<sup>[12,13]</sup> Here, we report a new strategy for creating protein-based (nano)materials that circumvent this limitation and preserve the unique molecular properties of their building blocks. This approach is based on genetically fusing various protein building blocks to monomeric streptavidin and exploiting the propensity of streptavidin monomers to self-assemble themselves into stable tetramers.<sup>[14,15]</sup>

Streptavidin monomers (SM) are known to form tetramers<sup>[16–21]</sup> of high thermal stability<sup>[22]</sup> that could potentially serve as hubs/nodes in supramolecular networks and materials. However, in general, proteins with high thermal stability not always display high mechanical strength.<sup>[23,24]</sup> In addition, it is presently unknown whether attaching large polypeptide chains to SMs will compromise the ability of SMs to assemble into tetramers. Even though numerous experimental and computational studies addressed the strength of the

interaction between biotin and avidin/streptavidin,<sup>[25–33]</sup> to the best of our knowledge, none directly investigated the mechanical strength of streptavidin itself. To evaluate whether streptavidin can be a useful cross-linker for protein-based materials, we used protein engineering to create polypeptides terminating with monomeric streptavidin, and used atomic force microscopy (AFM) to visualize streptavidin-based complexes and evaluated their tensile strength.

We genetically fused streptavidin monomers to two protein constructs with different mechanical properties. The first construct was composed of a streptavidin monomer and six tandem repeats of I27 domain of titin<sup>[34–38]</sup> connected to its N-terminus, I27<sub>6</sub>-SM (Figure 1a, 1b and 2a). I27 domains are mechanically strong (unfolding force at the speed of 500 nm/s is 200 pN), and provide a unique mechanical unfolding finger-print.<sup>[37–42]</sup> The second construct (Figure 3a) was composed of a streptavidin monomer and an N-terminal handle composed of three staphylococcal nuclease (SNase) modules interspersed with three I27 domains. SNase domains were recently shown to produce regular unfolding forces of 20–30 pN.<sup>[42]</sup>

I27-streptavidin and I27-SNase-streptavidin chimeras were expressed in *E coli* and purified as tetramers (Supporting Information). AFM images clearly revealed (I27<sub>6</sub>-SM)<sub>4</sub> structures in which streptavidin formed a central hub with four protruding I27<sub>6</sub> arms (Figure 1e). Based on protein gel analysis (Figure S1–S3) and AFM images, we conclude that SMs, functionalized with tandem I27 and SNase repeats, correctly assemble into uniform tetramer structures which also preserve their ability to bind biotins<sup>[15]</sup> (Figure 1d and Figure S4).

We used single molecule atomic force spectroscopy<sup>[43,44]</sup> to determine the mechanical strength of streptavidin tetramers (Figure 2a). Based on the design of the I27-streptavidin chimera (Figure 1b and 2a), we can be absolutely certain that a single streptavidin tetramer has been stretched when we record at least 7 (up to 12) characteristic unfolding force peaks of I27 domains. For example, the top trace in Figure 2b captured the unfolding of ten I27 domains and the bottom trace revealed eleven characteristic I27 force peaks. Following the I27 force peaks, both traces also captured a large force peak (black circles in Figure 2b) before the measured force dropped to zero. This large force peak could be due to the rupture of streptavidin or due to detachment of the molecule from the AFM tip or the substrate. From these and other similar measurements, we conclude that the strength of streptavidin tetramers is equal or greater to the last force peak measured by AFM. However, to differentiate streptavidin rupture events from protein detachment events, we performed similar force spectroscopy measurements on I27 constructs without SMs (Figure S6).

The probability density function (pdf) of detachment events for I27 handles is compared in Figure 2c (gray dashed line) with the pdf for last force peaks of the streptavidin tetramer containing constructs (black solid line in Figure 2c). The histograms of both types of events are compared in Figure S8a. While the pdf of detachment forces displays a long tail at forces as high as 700 pN, the pdf of last force peaks of streptavidin constructs ends at 500 pN and displays a pronounced hump at around 400 pN which is absent in the detachment pdf. We conclude that this hump is produced by streptavidin rupture events and estimate the strength of the streptavidin tetramers at our pulling conditions to be 400–500 pN. Similar conclusions can be obtained by analyzing respective histograms (Figure S8a).

By using I27 domains for the identification of single molecule measurements, we obviously selected only those AFM recordings in which the measured tension exceeded the unfolding threshold force of I27, ~200 pN. Therefore, any events in which streptavidin tetramers could break at forces lower than 200 pN (if any) would have been missed. To identify rupture events that could possibly occurred at lower forces, we used the second construct, [(I27-

SNase)<sub>3</sub>-SM]<sub>4</sub>, for force spectroscopy measurements (Figure 3a). Figure 3b shows typical AFM force-extension curves obtained on [(I27-SNase)<sub>3</sub>-SM]<sub>4</sub>. Interestingly, around 70% of single molecule force-extension curves contained 4 (up to 6) characteristic unfolding force peaks of SNase with recordings ending before any I27 modules unfolded (top panel of Figure 3b). About 30% of the recordings contained I27 unfolding force peaks (bottom panel of Figure 3b) and very rarely (approximately 5% of recordings) they displayed a force greater than 300 pN. Never did the force exceed 500 pN.

As before, we analyzed the last unfolding force peaks in all single molecule recordings of [(I27-SNase)<sub>3</sub>-SM]<sub>4</sub> and showed their pdf (black solid line in Figure 3c; the histograms are shown in Figure S8b). We also performed single molecule force spectroscopy experiments on the SNase-I27 construct without SMs (Figure S7) and show the pdf of detachment force peaks in Figure 3c (gray dashed line). Surprisingly, at around 100 pN, the streptavidin pdf is significantly greater as compared to the detachment pdf. We conclude that the origin of this difference is caused by numerous streptavidin rupture events which occur at forces around 100 pN that were missed in measurements using I27 handles.

What is the origin of these high and low rupture forces? Structural studies revealed that identical streptavidin monomers (A, B, C and D) are assembled into tetramers as dimers of dimers<sup>[20,21]</sup> (Figure 4a). Based on the crystal structure of streptavidin<sup>[20,21]</sup>, monomers are tightly associated into dimers<sup>[21]</sup> due to strong interactions across the A and B (AB) and C and D (CD) interfaces with large contact areas (~16 nm<sup>2</sup>), which involve 17 hydrogen bonds (H-bonds) and other non-covalent interactions.<sup>[45]</sup> Relatively weak interactions exist in cross-interfaces between monomers A and D (AD) and B and C (BC) with only two H-bonds and other interactions, involving relatively small contact areas (~5 nm<sup>2</sup>).<sup>[21,45]</sup> Even weaker interactions occur across A and C and B and D interfaces with a contact area of less than ~2 nm<sup>2</sup>.<sup>[45]</sup>

This analysis suggests that the internal interfaces within a streptavidin tetramer may have different mechanical strengths and, because of this anisotropy, the mechanical strength of a streptavidin tetramer may actually depend, in a complicated fashion, on the pulling geometry. Taken together, our AFM results suggest that when using I27 handles, we mainly probed rupture events between streptavidin monomers such as AB or CD (Figure 4). These events likely rupture 17 H-bonds and therefore, require large stretching forces in excess of 300 pN at a pulling speed of 500 nm/s. However, when exploiting the unfolding signature of SNase, we probed all possible rupture events within the streptavidin tetramer that occur between monomers (AB or CD) and dimers (AB and CD). The latter likely involves the rupture of only 4 H-bonds and therefore, requires a significantly lower stretching force of approximately 100 pN. The fact that we only observed a few high force rupture events using SNase-I27 handles strongly suggests that dimer rupture events must occur more frequently than monomer rupture events. This is consistent with the random attachment of protein handles to the AFM probe and substrate that favors dimer separation along the  $F_2$  or  $F_3$  directions over the  $F_1$  direction inducing monomer separation in a 2:1 ratio (Figure 4b). We note that the strength of the dimer-dimer interface in streptavidin is comparable or even weaker (at the examined stretching rates) than the biotin-streptavidin unbinding force that was reported to range from 100 pN to 450 pN when measured by AFM<sup>[29,31]</sup>. The mechanical strength of the monomer-monomer interface (around 400 pN) is greater than the unfolding forces of most proteins studied so far. Therefore, this interface will likely be strong enough to support a material with high tensile strength. It should be possible to reinforce the dimer-dimer interface in streptavidin beyond its current tensile strength of approximately 100 pN, by introducing inter-subunit crosslinks.<sup>[46,47]</sup>

We note that using I27 and/or SNase domains as polypeptide linkers will produce highly extensible materials which dissipate a significant amount of stretching energy.<sup>[3,13]</sup> In our approach, I27 domains can be easily replaced at the DNA level, with other polypeptides that may provide other desirable elastic properties such as a large stretch ratio with minimal energy dissipation (for example, repeat proteins based nano-springs; ref. 12 and 13). However, to create 2D or 3D materials based on streptavidin hubs, polypeptide linkers need to be further functionalized for second-level self-assembly. For example, the N-terminus of these polypeptides can be preceded by AviTag<sup>[48]</sup> to which biotin can be enzymatically added, or by *Strep*-tag II<sup>[49]</sup> engineered at the DNA level. Self-assembly can then be achieved by mixing the biotinylated tetramers with soluble streptavidin, or using *Strep*-tag terminated hubs with soluble *Strep*-Tactin<sup>[50,51]</sup> (Figure S9a and S9b). Alternatively, the N-terminus of polypeptide linkers can be fused with the FKBP12 polypeptide and self-assembly would be achieved in the presence of FK1012, a chemical inducer of dimerization for FKBP12 domains<sup>[52]</sup> (Figure S9c). Because, in our approach, biotin binding sites are still available on streptavidin hubs (Figure 1d and Figure S4), they also can be exploited for further crosslinking strategies or to connect streptavidin mediated networks to other structures. For instance, biotinylated phosphatidylserines in a lipid bilayer could anchor streptavidin hubs to large unilamellar liposomes to form 2D networks on their surface. Such networks would support the structure of liposome-based “artificial cells”, in a fashion similar to that of the red blood cell cytoskeleton.

## Experimental Section

To prepare I27<sub>6</sub>-SM and (SNase-I27)<sub>3</sub>-SM plasmids, core streptavidin genes (residues 13-139) were fused into the 7th and 8th positions of pAFM1-8<sup>[53]</sup> and pAFM1-8(SNase 2, 4, 6)<sup>[42]</sup> plasmids. Self-assembled (I27<sub>6</sub>-SM)<sub>4</sub> and [(SNase-I27)<sub>3</sub>-SM]<sub>4</sub> and were purified using Ni-NTA column and 100 kDa centrifugal filter devices. For AFM imaging, 1.5 kb single-end biotinylated DNA and (I27<sub>6</sub>-SM)<sub>4</sub> were premixed with a molar ratio of 2:1, then incubated on mica for imaging in air. All force-extension measurements were carried out on custom-built AFM instruments as described previously.<sup>[13,54,55]</sup> Probability density functions were calculated by the kernel density estimation<sup>[56]</sup> using custom-written codes in Python. More details on the experimental methods are included in the Supporting Information.

## Supplementary Material

Refer to Web version on PubMed Central for supplementary material.

## Acknowledgments

We gratefully thank to Prof. P. Stayton (University of Washington, Seattle, WA) and Prof. J. Clarke (University of Cambridge, Cambridge, UK) for providing core streptavidin plasmids and pAFM 1-8 plasmids, respectively. We thank members of Prof. Marszalek’s group for helpful discussion. This work was supported in part by the National Institutes of Health’s grant GM079563. VB is a HHMI Investigator.

## References

1. Smith BL, Schaffer TE, Viani M, Thompson JB, Frederick NA, Kindt J, Belcher A, Stucky GD, Morse DE, Hansma PK. *Nature*. 1999; 399:761–763.
2. Langer R, Tirrell DA. *Nature*. 2004; 428:487–492. [PubMed: 15057821]
3. Lv S, Dudek DM, Cao Y, Balamurali MM, Gosline J, Li HB. *Nature*. 2010; 465:69–73. [PubMed: 20445626]
4. Li HB, Cao Y. *Acc Chem Res*. 2010; 43:1331–1341. [PubMed: 20669937]
5. Messersmith PB. *Science*. 2008; 319:1767–1768. [PubMed: 18369126]

6. Lee H, Lee BP, Messersmith PB. *Nature*. 2007; 448:338–341. [PubMed: 17637666]
7. Becker N, Oroudjev E, Mutz S, Cleveland JP, Hansma PK, Hayashi CY, Makarov DE, Hansma HG. *Nat Mater*. 2003; 2:278–283. [PubMed: 12690403]
8. de la Rica R, Matsui H. *Chem Soc Rev*. 2010; 39:3499–3509. [PubMed: 20596584]
9. Stupp SI. *Nano Lett*. 2010; 10(12):4783–4786.
10. Vogel V, Hess H. *Lect Notes Phys*. 2007; 711:367–383.
11. Tirrell DA, Maskarinec SA. *Curr Opin Biotechnol*. 2005; 16:422–426. [PubMed: 16006115]
12. Lee G, Abdi K, Jiang Y, Michaely P, Bennett V, Marszalek PE. *Nature*. 2006; 440:246–249. [PubMed: 16415852]
13. Kim M, Abdi K, Lee G, Rabbi M, Lee W, Yang M, Schofield CJ, Bennett V, Marszalek PE. *Biophys J*. 2010; 98:3086–3092. [PubMed: 20550922]
14. Sano T, Cantor CR. *Bio-Technol*. 1991; 9:1378–1381.
15. Murray MN, Hansma HG, Bezanilla M, Sano T, Ogletree DF, Kolbe W, Smith CL, Cantor CR, Spengler S, Hansma PK, Salmeron M. *Proc Natl Acad Sci USA*. 1993; 90:3811–3814. [PubMed: 8483898]
16. Sano T, Cantor CR. *Methods Enzymol*. 2000; 326:305–311. [PubMed: 11036649]
17. Chaiet L, Wolf FJ. *Arch Biochem Biophys*. 1964; 106:1–5. [PubMed: 14217155]
18. Argarana CE, Kuntz ID, Birken S, Axel R, Cantor CR. *Nucleic Acids Res*. 1986; 14:1871–1882. [PubMed: 3951999]
19. Pahler A, Hendrickson WA, Kolks MA, Argarana CE, Cantor CR. *J Biol Chem*. 1987; 262:13933–13937. [PubMed: 3654648]
20. Hendrickson WA, Pahler A, Smith JL, Satow Y, Merritt EA, Phizackerley RP. *Proc Natl Acad Sci USA*. 1989; 86:2190–2194. [PubMed: 2928324]
21. Weber PC, Ohlendorf DH, Wendoloski JJ, Salemme FR. *Science*. 1989; 243:85–88. [PubMed: 2911722]
22. Gonzalez M, Argarana CE, Fidelio GD. *Biomol Eng*. 1999; 16:67–72. [PubMed: 10796986]
23. Junker JP, Hell K, Schlierf M, Neupert W, Rief M. *Biophys J*. 2005; 89:L46–L48. [PubMed: 16183885]
24. Oberhauser AF, Badilla-Fernandez C, Carrion-Vazquez M, Fernandez JM. *J Mol Biol*. 2002; 319:433–447. [PubMed: 12051919]
25. Florin EL, Moy VT, Gaub HE. *Science*. 1994; 264:415–417. [PubMed: 8153628]
26. Moy VT, Florin EL, Gaub HE. *Science*. 1994; 266:257–259. [PubMed: 7939660]
27. Wong SS, Joselevich E, Woolley AT, Cheung CL, Lieber CM. *Nature*. 1998; 394:52–55. [PubMed: 9665127]
28. Merkel R, Nassoy P, Leung A, Ritchie K, Evans E. *Nature*. 1999; 397:50–53. [PubMed: 9892352]
29. Lee CK, Wang YM, Huang LS, Lin SM. *Micron*. 2007; 38:446–461. [PubMed: 17015017]
30. Chilkoti A, Boland T, Ratner BD, Stayton PS. *Biophys J*. 1995; 69:2125–2130. [PubMed: 8580356]
31. Zlatanova J, Lindsay SM, Leuba SH. *Progr Biophys Mol Biol*. 2000; 74:37–61.
32. Izrailev S, Stepaniants S, Balsera M, Oono Y, Schulten K. *Biophys J*. 1997; 72:1568–1581. [PubMed: 9083662]
33. Grubmuller H, Heymann B, Tavan P. *Science*. 1996; 271:997–999. [PubMed: 8584939]
34. Maruyama K. *FASEB J*. 1997; 11:341–345. [PubMed: 9141500]
35. Wang K. *Adv Biophys*. 1996; 33:123–134. [PubMed: 8922107]
36. Labeit S, Kolmerer B. *Science*. 1995; 270:293–296. [PubMed: 7569978]
37. Li HB, Linke WA, Oberhauser AF, Carrion-Vazquez M, Kerkvliet JG, Lu H, Marszalek PE, Fernandez JM. *Nature*. 2002; 418:998–1002. [PubMed: 12198551]
38. Rief M, Gautel M, Oesterhelt F, Fernandez JM, Gaub HE. *Science*. 1997; 276:1109–1112. [PubMed: 9148804]
39. Williams PM, Fowler SB, Best RB, Toca-Herrera JL, Scott KA, Steward A, Clarke J. *Nature*. 2003; 422:446–449. [PubMed: 12660787]

40. Carrion-Vazquez M, Oberhauser AF, Fowler SB, Marszalek PE, Broedel SE, Clarke J, Fernandez JM. *Proc Natl Acad Sci USA*. 1999; 96:3694–3699. [PubMed: 10097099]
41. Marszalek PE, Lu H, Li HB, Carrion-Vazquez M, Oberhauser AF, Schulten K, Fernandez JM. *Nature*. 1999; 402:100–103. [PubMed: 10573426]
42. Wang CC, Tsong TY, Hsu YH, Marszalek PE. *Biophys J*. 2011; 100:1094–1099. [PubMed: 21320455]
43. Liang J, Fernandez JM. *ACS Nano*. 2009; 3:1628–1645. [PubMed: 19572737]
44. Puchner EM, Gaub HE. *Curr Opin Struct Biol*. 2009; 19:605–614. [PubMed: 19822417]
45. Wu SC, Wong SL. *J Biol Chem*. 2005; 280:23225–23231. [PubMed: 15840576]
46. Chilkoti A, Schwartz BL, Smith RD, Long CJ, Stayton PS. *Bio-Technol*. 1995; 13:1198–1204.
47. Reznik GO, Vajda S, Smith CL, Cantor CR, Sano T. *Nat Biotechnol*. 1996; 14:1007–1011. [PubMed: 9631041]
48. Beckett D, Kovaleva E, Schatz PJ. *Protein Sci*. 1999; 8:921–929. [PubMed: 10211839]
49. Schmidt TGM, Koepke J, Frank R, Skerra A. *J Mol Biol*. 1996; 255:753–766. [PubMed: 8636976]
50. Korndorfer IP, Skerra A. *Protein Sci*. 2002; 11:883–893. [PubMed: 11910031]
51. Voss S, Skerra A. *Protein Eng*. 1997; 10:975–982. [PubMed: 9415448]
52. Keenan T, Yaeger DR, Courage NL, Rollins CT, Pavone ME, Rivera VM, Yang W, Guo T, Amara JF, Clackson T, Gilman M, Holt DA. *Bioorg Med Chem*. 1998; 6:1309–1335. [PubMed: 9784872]
53. Steward A, Toca-Herrera JL, Clarke J. *Protein Sci*. 2002; 11:2179–2183. [PubMed: 12192073]
54. Marszalek PE, Oberhauser AF, Pang YP, Fernandez JM. *Nature*. 1998; 396:661–664. [PubMed: 9872313]
55. Rabbi, M.; Marszalek, PE. *Single Molecule Techniques: A Laboratory Manual*. Selvin, PR.; Ha, T., editors. Cold Spring Harbor Laboratory Press; 2008. p. 371-394.
56. Scott, DW. *Multivariate Density Estimation: Theory, Practice, and Visualization*. John Wiley & Sons, Inc; New York: 1992.

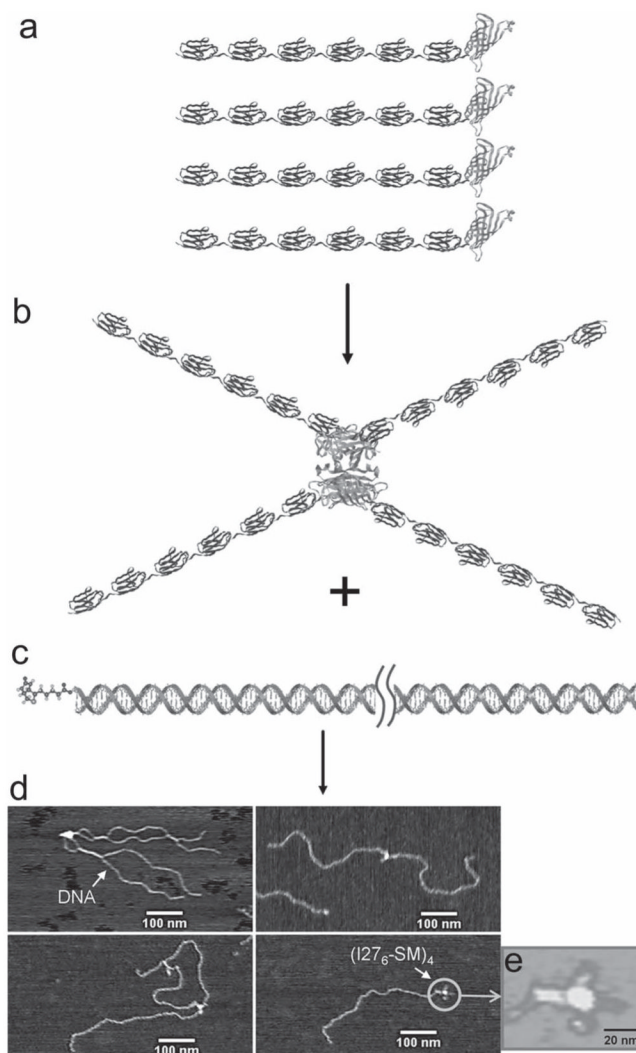


**Figure 1.** Designing well-defined protein-based building blocks for constructing self-assembled nanostructured materials. a) A schematic of  $(I27-SM)_1$  building blocks. b) A schematic of the structure of  $(I27_6-SM)_4$  created during protein expression in *E.coli* through self-assembly of monomeric streptavidin. c) A schematic of 1.5kb single-end biotinylated DNA. d) AFM images of  $(I27_6-SM)_4$  incubated with biotinylated DNA (see also Figure S4). e) High-resolution AFM image of  $(I27_6-SM)_4$  shows a structure that is similar to the schematic illustration in (b). The measured length of  $\sim 50$  nm from one arm to another matches the expected length of the complex. The total length of the intact 12 I27 and streptavidin tetramer is  $\sim 53$  nm based on crystal structures of both proteins: a single I27 =  $\sim 4$  nm (PDB: 1TIT) and a core streptavidin =  $\sim 5$  nm (PDB: 1MK5).

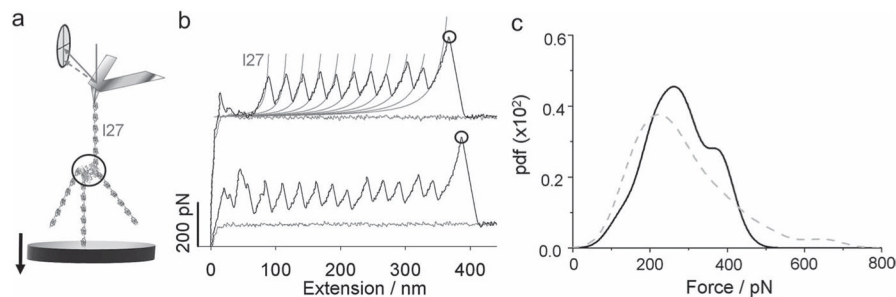


**Figure 2.**

Strong intermolecular forces of the streptavidin tetramer. a) A schematic illustrates AFM pulling experiments on  $(I27_6-SM)_4$ . b) Examples of force-extension curves display regular patterns of unfolding I27 domains followed by a large force peak (black circles) corresponding to rupture of streptavidin tetramers or detachment of the complex from the substrate or the AFM tip. Thin gray lines are WLC model fits to the curve with contour length increments ( $L_c$ ) of 29.5 nm and persistent length ( $p$ ) of 0.4 nm. c, The comparison of pdfs of last force peaks from (b) (black solid line,  $n = 110$ ) and detachment forces of I27<sub>7</sub> constructs without streptavidin (gray circle in Figure S6; gray dashed line in Figure 2c,  $n = 120$ ). The data in Figure 2c and 3c were collected at the AFM pulling speed of 500 nm/s.



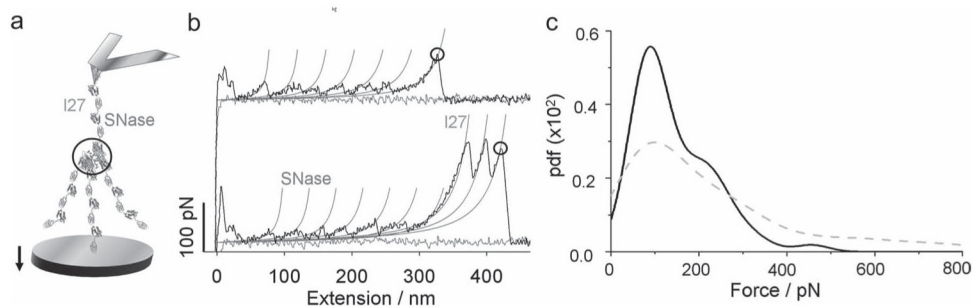


**Figure 3.** Mechanical anisotropy of the streptavidin tetramer. a) A schematic illustrates the AFM experimental geometry of the  $[(\text{SNase-I27})_3\text{-SM}]_4$  construct. b) Examples of force-extension curves show 6 unfolding force peaks of SNase modules without (top panel) or with unfolding force peaks of I27 domains (bottom panel). Thin gray lines are WLC model fits to both sets of curves with  $L_c = 48$  nm (SNase, top), 45 nm (SNase, bottom) and 30 nm (I27, bottom), and  $p = 0.7$  nm (SNase) and 0.4 nm (I27). c) The comparison of pdfs which were obtained based on the last force peaks from (b) and similar recordings (black circles in (b); black solid line,  $n = 56$ ) and detachment forces of I27-(SNase-I27)<sub>3</sub> constructs (gray circle in Figure S7; gray dashed line in Figure 3c,  $n = 160$ ).

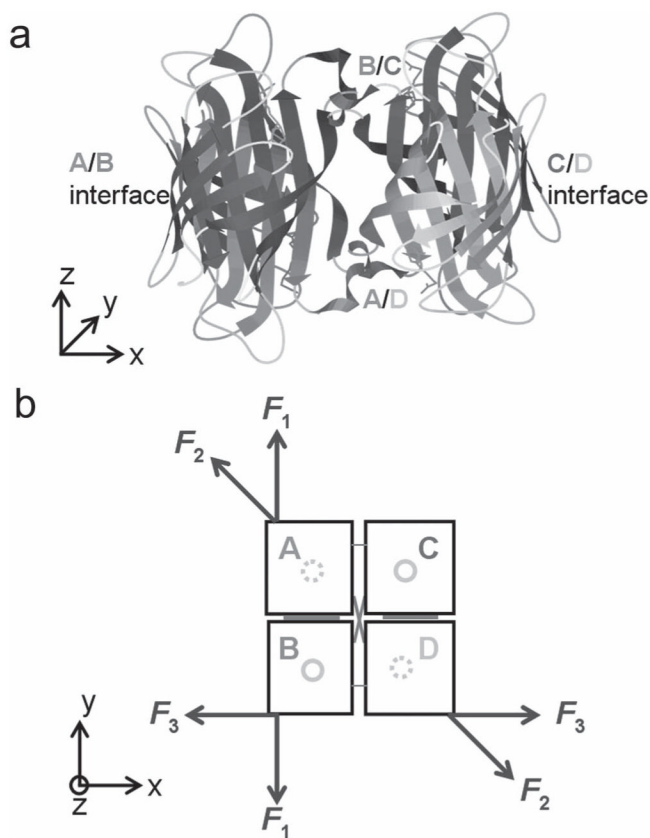


**Figure 4.** Three possible AFM pulling geometries on streptavidin tetramer. a) The crystal structure of streptavidin tetramer (PDB: 1MK5). b) When polypeptide building blocks are fused onto the N-terminus of streptavidin tetramers, three pulling geometries are possible during AFM-based force spectroscopy measurements. Gray circles indicate biotin binding sites (solid circles for top binding sites and dashed circles for the bottom sites). Gray shades represent contact areas between monomers by H-bonds and/or non-covalent interactions.